

An improved prescription for merger time-scales from controlled simulations

Á. Villalobos^{1*}, G. De Lucia¹, S. Weinmann², S. Borgani^{1,3,4}, and G. Murante¹

¹*INAF - Astronomical Observatory of Trieste, via G.B. Tiepolo 11, 34143 Trieste, Italy*

²*Leiden Observatory, Leiden University, P.O. Box 9513, 2300 RA Leiden, The Netherlands*

³*University of Trieste, Department of Physics, via Valerio 2, 34127 Trieste, Italy*

⁴*INFN - National Institute for Nuclear Physics, via Valerio 2, 34127 Trieste, Italy*

Accepted — . Received — ; in original form —

ABSTRACT

We compare three analytical prescriptions for merger times available from the literature to simulations of isolated mergers. We probe three different redshifts, and several halo concentrations, mass ratios, orbital circularities and orbital energies of the satellite. We find that prescriptions available in the literature significantly under-predict long timescales for mergers at high redshift. We argue that these results have not been highlighted previously either because the evolution of halo concentration of satellite galaxies has been neglected (in previous isolated merger simulations), or because long merger times and mergers with high initial orbital circularities are under-represented (for prescriptions based on cosmological simulations). Motivated by the evolution of halo concentration at fixed mass, an explicit dependence on redshift added as $t_{\text{merger}}^{\text{mod}}(z) = (1+z)^{0.44} t_{\text{merger}}$ to the prescription based on isolated mergers gives a significant improvement in the predicted merger times up to $\sim 20 t_{\text{dyn}}$ in the redshift range $0 \leq z \leq 2$. When this modified prescription is used to compute galaxy stellar mass functions, we find that it leads up to a 25 per cent increase in the number of low mass galaxies surviving at $z=0$, and a 10 per cent increase for more massive galaxies. This worsens the known over-prediction in the number of low mass galaxies by hierarchical models of galaxy formation.

Key words: galaxies: evolution – galaxies: structure – galaxies: kinematics and dynamics – galaxies: interactions – methods: N-body simulations

1 INTRODUCTION

Galaxies orbiting in dense environments, such as groups or clusters, suffer a continuous loss of energy and angular momentum under the effect of dynamical friction against the medium of their parent halo. Because of this, galaxies on bound orbits spiral-in towards the densest regions of their local environment on a given timescale. This merger timescale t_{merger} is usually modelled as a function of the dynamical timescale of the main halo, t_{dyn} , the galaxy-main halo mass ratio, and the orbital energy and circularity of the infalling galaxy. All of these quantities are considered at the time a galaxy crosses the virial radius of the main halo along its infalling orbit. Merger timescales are defined as the time until the galaxy has lost a significant fraction of either its initial mass via tidal stripping, or of its initial orbital angular momentum.

Accurate estimates of how long a galaxy survives within

a halo while being affected by dynamical friction are fundamental for theoretical studies of galaxy evolution. Indeed, merger times play a key role in the evolution of galaxies' stellar masses, morphologies, colours, and gas content (e.g. Cox et al. 2008; De Lucia et al. 2010, 2011).

In recent years, Boylan-Kolchin et al. (2008, B08), Jiang et al. (2008, J08), and McCavana et al. (2012, M12) have provided different prescriptions to estimate merger timescales. All three prescriptions are variations of the analytic description derived by Chandrasekhar (1943) for the drag force suffered by a point mass object as it moves through a uniform background medium of less massive particles (see Binney & Tremaine 1987). The aforementioned prescriptions are obtained either by simulating single isolated mergers at $z=0$ that probe a given parameter space, or by collecting a sample of mergers from cosmological simulations within a given redshift range. In this paper, we compare these prescriptions with controlled simulations of isolated galaxies being accreted onto a group-like halo at three redshift epochs. We explore several halo concentrations in

* villalobos@oats.inaf.it

Table 1. Properties of group environments and galaxies.

	“z=0”	“z=1”	“z=2”	
Group DM halo				
Virial mass	9.9	9.9	9.9	($\times 10^{12} M_{\odot}$)
Virial radius	555.94	329.19	226.09	(kpc)
Concentration	9.74	4.87	3.25	
Circular velocity	276.97	360.07	434.62	(km s^{-1})
Number particles	5.5	5.5	5.5	($\times 10^5$)
Softening	0.55	0.32	0.22	(kpc)
Group stellar spheroid				
Mass	1	1	1	($\times 10^{11} M_{\odot}$)
Scale radius	3.24	1.91	1.31	(kpc)
Number particles	2.5	2.5	2.5	($\times 10^5$)
Softening	0.1	0.06	0.04	(kpc)
Galaxy DM halo				
Virial mass	2.97-39.6	2.47-34.6	2.97-9.9	($\times 10^{11} M_{\odot}$)
Virial radius	172.7-409.6	96.2-231.9	70.2-104.9	(kpc)
Concentration	15.36-10.97	7.87-5.58	5.12-4.38	
Number particles	2.5	2.5	2.5	($\times 10^5$)
Softening	0.35	0.26	0.19	(kpc)
Galaxy stellar disc				
Mass	2.8	1.42	0.72	($\times 10^{10} M_{\odot}$)
Scale-length	3.5	1.65	0.9	(kpc)
Number particles	5	5	5	($\times 10^4$)
Softening	0.05	0.012	0.007	(kpc)

both systems, merger mass ratios, and orbital parameters of accreted galaxies. Our main goal is to determine whether the implicit dependency of these prescriptions on redshift (via t_{dyn}) is enough to account for relevant properties of haloes that are known to evolve with cosmic time, such as halo concentration.

The layout of this paper is as follows: Section 2 describes the set-up of our experiments; Section 3 describes our results, comparing them to models from the literature; in Section 4 we discuss our results and in Section 5 we give our conclusions.

2 SET-UP OF NUMERICAL EXPERIMENTS

We have carried out 50 simulations of isolated mergers between a single galaxy and a larger main halo, in order to quantify their merger timescales. Similarly to B08, our basic strategy is to release a single disc galaxy at a time, on a bound orbit, from the virial radius of the main halo and study the evolution of its mass content and orbital angular momentum as it is dragged towards the centre of the halo. Our simulations cover the time span since a galaxy is released from the virial radius of the main halo until it is either disrupted or it has exhausted its initial orbital angular momentum (see Section 3.1).

Each main halo is modelled as a N -body self-consistent multi-component system, where the DM halo follows a NFW density profile (Navarro et al. 1997):

$$\rho_{\text{halo}}(r) = \frac{\rho_s}{(r/r_s)(1+r/r_s)^2}, \quad (1)$$

where ρ_s is a characteristic scale density and r_s a scale radius. Additionally, a spherical stellar component, resembling a central galaxy, is located at the halo centre, and its mass follows a Hernquist density profile (Hernquist 1990):

$$\rho_*(r) = \frac{M_*}{2\pi} \frac{a_*}{r(r+a_*)^3}, \quad (2)$$

where M_* is the stellar mass and a_* is the scale radius. Similarly, each galaxy is also modelled as a self-consistent multi-component system, formed by a stellar disc embedded in a DM halo. The stellar mass in discs follows an exponential density profile:

$$\rho_{\text{disc}}(R, z) = \frac{M_{\text{disc}}}{8\pi R_{\text{D}}^2 z_{\text{D}}} \exp\left(-\frac{R}{R_{\text{D}}}\right) \text{sech}^2\left(\frac{z}{2z_{\text{D}}}\right), \quad (3)$$

where M_{disc} is the disc mass, R_{D} is the exponential scale-length, and z_{D} is the exponential scale-height. The DM halo of galaxies is also assumed to follow a NFW profile. All DM haloes in our simulations are initially spherical, do not rotate, and the structure of their inner region has been adiabatically contracted to account for the growth of the baryonic component (see Villalobos & Helmi 2008, for details).

The initial orbital parameters of discs are chosen to be consistent with distributions of orbital parameters of infalling substructures, obtained from cosmological simulations (e.g., Benson 2005; Wetzel 2011). In this paper, we focus on the most likely orbital circularity of infalling substructures, and on the extreme values of the distributions.

The initial conditions of our isolated mergers are placed in a simplified context of three different redshift epochs, “z=0”, “z=1” and “z=2”. In this context, the *initial* structure of DM haloes is defined by both the virial over-density $\Delta_{\text{vir}}(z)$ (Bryan & Norman 1998) and the halo concentration $c(M_{\text{vir}}, z)$.¹ Note that during the simulations, a main halo *only* interacts with a single disc galaxy, and does not accrete additional mass. As for the evolution of halo concentration, we adopt $c(M_{\text{vir}}, z) \propto (1+z)^{-1}$ (Bullock et al. 2001).

At all three redshifts, main haloes have a mass of $10^{13} M_{\odot}$. This choice is based on the mass range reported by McGee et al. (2009) and De Lucia et al. (2012), where significant environmental effects on galaxies must take place (see also Berrier et al. 2009). We have kept fixed both the mass and scale-lengths of stellar discs, while covering a range of masses and radii of the DM haloes in which they are embedded (see below). The stellar-to-DM mass ratios of disc galaxies are consistent with stellar-to-DM mass relations from both observations and theoretical studies (Behroozi et al. 2010; Guo et al. 2010; Moster et al. 2010). Table 1 lists the structural parameters of main haloes and disc galaxies. Table 2 provides the range of the parameter space covered by our experiments. These parameters delimit the validity of our results. Note that our experiments do not include cases where $c_{\text{host}} \sim c_{\text{sat}}$ which would be relevant in the case of major mergers.

We have carried out test simulations to ensure that our results are not affected by numerical resolution. All simulations were run using GADGET-3 (Springel 2005).

3 RESULTS

3.1 Definition of “merger”

As a galaxy orbits within a halo, it gradually loses orbital energy and orbital angular momentum due to dynamical friction (mainly) against the medium of the larger halo. As its orbit decays towards the densest region of the halo, a

¹ We assume $\Omega_{m,0} = 0.3$, $\Omega_{\Lambda} = 0.7$ and $H_0 = 70 \text{ km s}^{-1} \text{ Mpc}^{-1}$.

Table 2. Ranges of parameters explored by the experiments.

z (1)	$M_{\text{host}}/M_{\text{sat}}$ (2)	η (3)	$r_c(E)/r_{\text{vir}}$ (4)	t_{DM} (5)	t_{J} (6)	t_{stars} (7)
0	2.5–33.33	0.21–0.91	0.91–1.94	4.8–26.5	4.8–28.5	5.3–29
1	2.86–40	0.21–0.9	1.01–1.97	3.2–22	3.7–26	4.2–26
2	10–33.33	0.55	1.06–1.16	2.5–10	3.5–22	4–24

(1) Redshift. (2) Mass ratio of each merger. (3) Initial orbital circularity of the satellite, in units of $V_c(r_{\text{vir}})$. (4): Initial orbital energy of the satellite, expressed in terms of the radius r_c of a circular orbit with the same orbital energy E , in units of r_{vir} . (5): merger time computed when only 5 per cent of the DM halo of a satellite remains bound, in Gyr. (6): merger time computed when only 5 per cent of the initial orbital angular momentum of a satellite is retained, in Gyr. (7): merger time computed when only 5 per cent of the stellar content of a satellite remains bound, in Gyr.

galaxy might also undergo mass loss via tidal stripping, especially at pericentric passages where tidal forces are stronger. Previous studies have used several criteria to define when a galaxy has “merged” with a larger halo. A galaxy is considered merged if either: (i) its remaining bound DM mass is 5 per cent of its initial value; or, (ii) the remaining orbital angular momentum is 5 per cent of its initial value; or, (iii) the remaining bound stellar mass is 5 per cent of its initial value. In general, all three definitions yield similar merger times, where usually $t_{\text{DM}} < t_{\text{J}} < t_{\text{stars}}$. In the rest of the paper, we adopt the definition of merger time as the minimum between t_{J} and t_{stars} . This corresponds to t_{J} in most of our experiments (e.g. see Fig. 1 in B08).

3.2 Comparison to previous models of merger times

We compare the merger times obtained from our simulations to the following models of merger timescales from the literature. B08 and M12, using isolated and cosmological simulations respectively, find:

$$\frac{t_{\text{merger}}^{\text{B08}}}{t_{\text{dyn}}} = A \frac{(M_{\text{host}}/M_{\text{sat}})^B}{\ln(1 + M_{\text{host}}/M_{\text{sat}})} e^{C\eta} \left[\frac{r_c(E)}{r_{\text{vir}}} \right]^D, \quad (4)$$

with the following best fitting parameters $(A, B, C, D) = (0.216, 1.3, 1.9, 1.0)$ for B08, and $(0.9, 1.0, 0.6, 0.1)$ for M12. J08, using cosmological hydro-dynamical simulations, find:

$$\frac{t_{\text{merger}}}{t_{\text{dyn}}} = \frac{0.94\eta^{0.6} + 0.6}{2 \times 0.43} \frac{M_{\text{host}}}{M_{\text{sat}}} \frac{1}{\ln[1 + (M_{\text{host}}/M_{\text{sat}})]}. \quad (5)$$

In all three models, $t_{\text{dyn}} = r_{\text{vir}}/V_c(r_{\text{vir}}) = \sqrt{2/\Delta(z)}/H(z)$, where the over-density $\Delta(z)$ and Hubble constant $H(z)$ vary as a function of redshift. Note that dynamical timescales do not depend on either halo mass or virial radius, but only on the cosmological parameters chosen. For the parameters used in this paper, the dynamical timescales in our simulations are $t_{\text{dyn}}(z=0)=1.9644$ Gyr, $t_{\text{dyn}}(z=1)=0.895$ Gyr, and $t_{\text{dyn}}(z=2)=0.5095$ Gyr.

Figure 1 (left) shows the predicted merger times from the B08, J08 and M12 prescriptions applied to our mergers. For experiments at “ $z=0$ ”, B08 offer accurate predictions at least up to $\sim 15 t_{\text{dyn}}$, independently of the merger definition used (Section 3.1). An analysis of predicted merger timescales as a function of the initial orbit of galaxies shows that the B08 model tends to slightly overestimate (underestimate) t_{merger} for galaxies with lower (higher) initial circularities (Figure 2). Also, B08 appears to be fine-tuned to

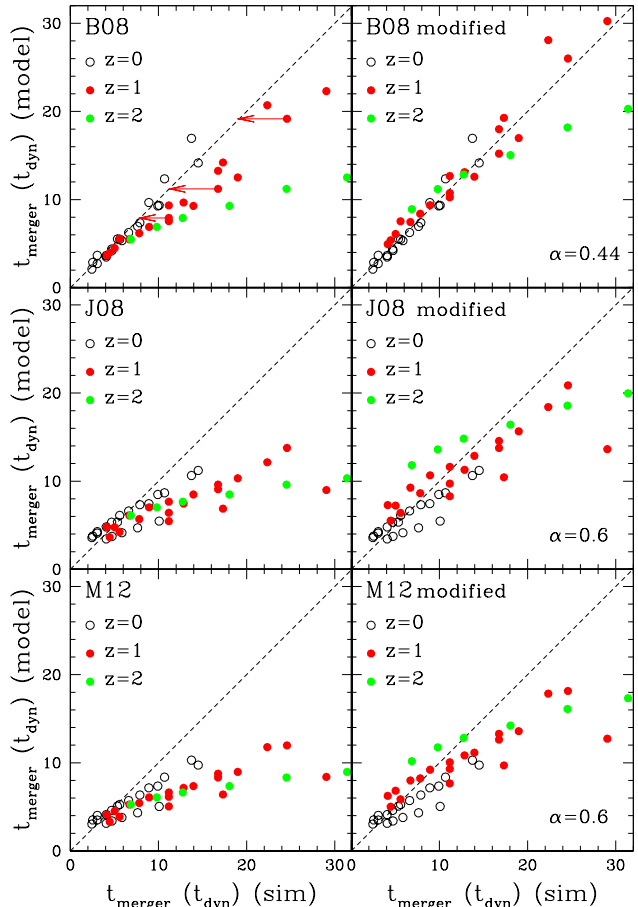


Figure 1. Left column: predictions of the B08, J08, M12 models applied to our experiments at “ $z=0$ ” (black), “ $z=1$ ” (red), and “ $z=2$ ” (green). Arrows indicate the improved accuracy of the prediction for selected experiments at “ $z=1$ ”, when mergers are resimulated with a higher initial concentration of the galaxies’ haloes. Right column: predictions of the respective modified models, $t_{\text{merger}}^{\text{mod}}(z) = (1+z)^\alpha t_{\text{merger}}$.

accurately predict merger timescales for galaxies infalling with the most likely orbital circularities ($\eta \sim 0.6$). The B08 model, applied to our experiments at “ $z=0$ ”, exhibits an overall scatter of ± 20 per cent across the range of explored circularities, decreasing to ± 10 per cent over different mass ratios at a fixed circularity. The high accuracy of the B08 prescription is not surprising, since it was obtained from simulations of isolated mergers at $z=0$, similar to those presented in this paper. However, for experiments at “ $z=1$ ” and “ $z=2$ ”, a comparable level of accuracy in the predictions is only reached up to $\sim 8 t_{\text{dyn}}$ (Figure 1, top-left). Beyond that limit, B08 systematically under-predicts merger times. Larger differences are observed for experiments with longer merger times and for those at higher redshift. As B08, J08 and M12 also significantly under-predict longer merger times, and increasingly so for mergers at higher redshift when compared to our controlled merger simulations. This implies that the implicit redshift dependence in all three models, from $t_{\text{dyn}}(z)$, is not enough to account for the measured evolution of merger timescales.

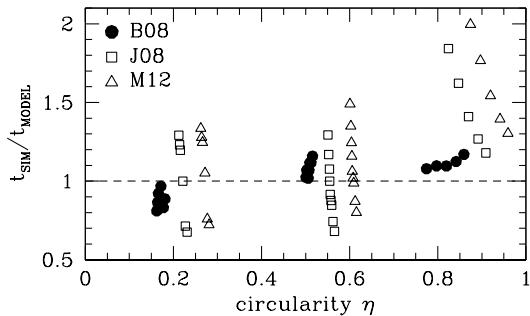


Figure 2. Comparison between predictions of the B08, J08 and M12 models applied to our experiments at “ $z=0$ ”, as a function of the initial orbital circularity of satellites. Predictions from B08 and M12 are shown with offsets $\eta-0.05$ and $\eta+0.05$, respectively, for clarity.

In general, we find that the J08 and M12 models yield similar predictions for our experiments at “ $z=0$ ”, although showing a significantly larger scatter in comparison to the B08 model (Figure 2). In spite of the larger scatter, J08 and M12 do predict accurately the median t_{merger} (for mergers of different mass ratios) for experiments with low and most likely initial orbital circularities. This is possibly a consequence of the fact that, in both studies, mergers are extracted from cosmological simulations, and so include a large number of radial mergers. Both models, however, under-predict the merger timescales in case of high circularities, which are associated to long merger times, showing an offset of ~ 55 per cent. The scatter associated to both J08 and M12 models is ± 35 per cent, for mergers with low and most likely initial orbital circularities.

We argue that the B08, J08 and M12 models under-predict long merger times at high redshift as a consequence of both neglecting the evolution of halo concentration in satellite, and under-sampling of long merger times.

3.2.1 Evolution of halo concentration in satellites

In order to study the effect of changes in the density profile of satellite haloes, we have resimulated three experiments at “ $z=1$ ”, increasing the concentration of their DM haloes. Specifically, we have given to those DM haloes a higher concentration as haloes of the same mass would have at “ $z=0$ ”. Arrows in Figure 1 (top-left) show that predictions from the B08 model become significantly more accurate in the case of mergers with more concentrated DM haloes.

A satellite with a higher concentration is expected to be more resilient against tidal disruption. Therefore, it will retain more of its mass, leading to a shorter merging timescale. Since the B08 model is obtained from isolated mergers at $z=0$, satellite haloes are assumed to have a too high concentration when the model is applied to mergers at $z>0$, which leads to shorter predicted merger times.

This result strongly suggests that the systematic under-prediction of longer merger timescales by the B08 model comes as a consequence of the evolution of halo concentration in our experiments [$c(M_{\text{vir}}, z) \propto (1+z)^{-1}$, Section 2], which is not included in their simulations. Note that the evolution of halo concentration also puts a strain on the validity of merger times models derived from the Chandrasekhar dy-

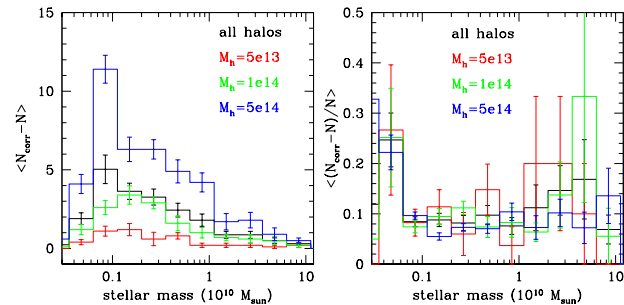


Figure 3. Left: difference between galaxy stellar mass functions using $t_{\text{merger}}^{\text{mod}}(z)$ and $t_{\text{merger}}^{\text{B08}}$ models, averaged over 10 haloes in each mass range: $5 \times 10^{13} M_{\odot}$, $10^{14} M_{\odot}$ and $5 \times 10^{14} M_{\odot}$ at $z=0$. Right: averaged fractional increase (in each galaxy stellar mass bin) associated to $t_{\text{merger}}^{\text{mod}}(z)$, with respect to the $t_{\text{merger}}^{\text{B08}}$ model.

namical friction formula (Chandrasekhar 1943), as they are applied to mergers of *extended* objects.

Motivated by the inverse proportionality between t_{merger} and c in our experiments, we introduce a modification to the B08 model in the form $t_{\text{merger}}^{\text{mod}}(z) = (1+z)^{\alpha} t_{\text{merger}}^{\text{B08}}$. We find that the inclusion of this modification, with $\alpha=0.44$, offers an improvement in the predicted merger timescales at least up to $\sim 20 t_{\text{dyn}}$ for mergers between $0 \leq z \leq 2$ (Figure 1, top-right).² Note however that a factor ~ 2 variation in concentration at fixed halo mass (Neto et al. 2007), implies a ~ 1.4 variation in t_{merger} .

In both J08 and M12, the evolution of halo concentration is already included in their cosmological simulations by construction. No details about the concentration of haloes are however discussed in these studies.

3.2.2 Under-sampling of long merger times

Even though cosmological simulations are statistically robust and provide a realistic context for studies of merger timescales, in general both long timescales ($>15 t_{\text{dyn}}$) and mergers with high circularities are severely under-represented. For instance, only mergers completed by $z=0$ and with orbital pericentres $\leq r_{\text{vir}}$ are considered in M12. As a consequence, this likely leads to inaccurate predictions of long merger timescales. Even though the motivation behind our modification does not apply to the J08 and M12 models (since evolution of halo concentration is included in their models by construction), our proposed modification does partially alleviate the disagreement between their predictions and our simulations, as shown in Figure 1. Note that B08 might also be affected by under-sampling given the relatively low number of long mergers their fitting formula is based on.

² The time dependence in this modification comes only indirectly through the median concentration-redshift relation.

4 DISCUSSION

We study the effect of our modification to the B08 model on the galaxy stellar mass functions for galaxies residing in haloes of different mass.

The galaxy stellar mass functions are computed by selecting from the Millennium simulation (Springel et al. 2005) 30 haloes in three mass ranges ($5 \times 10^{13} M_{\odot}$, $10^{14} M_{\odot}$, and $5 \times 10^{14} M_{\odot}$ at $z=0$). Following their main progenitors back in time, we extract all information about the galaxies residing in each halo and in its main progenitors, taking advantage of publicly available galaxy catalogues (De Lucia & Blaizot 2007). For each galaxy, we then store both its mass and that of its host halo at accretion time (i.e. the snapshot before it becomes a satellite for the first time). In the procedure, we take care of avoiding counting the same galaxy more than once. An orbital circularity is assigned randomly to each galaxy from distributions of orbital parameters obtained by Benson (2005). Then, both $t_{\text{merger}}^{\text{B08}}$ and $t_{\text{merger}}^{\text{mod}}(z)$ prescriptions are applied to each galaxy and its host. Finally, it is assumed that a galaxy has survived by $z=0$, if $t_{\text{merger}} > t_{\text{LB}}(z_{\text{accretion}})$, where t_{LB} is the look-back time at the redshift of accretion. As a first approximation, we assume that all surviving galaxies conserve their stellar mass since they were accreted. We also assume that the stellar mass of galaxies that do not survive is added to either the diffuse stellar component of the main halo, or to the central galaxy. This is clearly a strong simplification, since mergers between satellite galaxies within a main halo could also take place, altering the intermediate-mass region of the mass functions. We plan to study in a future work the consequences of the proposed modified model in the context of a more realistic galaxy formation model.

Figure 3 (left) shows the difference between mass functions using $t_{\text{merger}}^{\text{mod}}(z)$ and $t_{\text{merger}}^{\text{B08}}$ models, averaged over 10 haloes in each mass range. We find that the modification introduced leads to a larger number of lower mass satellites surviving at $z=0$, across all explored mass ranges. This comes as a natural consequence of the under-prediction of long merger timescales (associated to low mass satellites) at high redshift by the B08 model, as seen in Figure 1 (left).

Figure 3 (right) shows the fractional increase in the number of satellites within each galaxy stellar mass bin, due to the use of $t_{\text{merger}}^{\text{mod}}(z)$ with respect to the $t_{\text{merger}}^{\text{B08}}$ model. We find that satellites on the low mass end present the most significant fractional increase: ~ 25 per cent considering haloes in all mass ranges. On the other hand, more massive satellites show a rather constant (within the standard errors) fractional increase of ~ 10 per cent. Previous studies comparing observational data to predictions from semi-analytic models of galaxy evolution have found that these over-predict the number of faint galaxies (Weinmann et al. 2006; Liu et al. 2010). Our results suggest that this problem would worsen if more realistic models of merger timescales are employed.

By assuming that all the stellar content of merged galaxies contributes to the mass of central galaxies, we find that $t_{\text{merger}}^{\text{mod}}(z)$ leads to a mass reduction of ~ 10 per cent for the central galaxy, with respect to $t_{\text{merger}}^{\text{B08}}$. This is because there is less contribution from merged satellites, which would have longer survival times. This calculation assumes that the

initial mass of the central galaxy (i.e., before mergers take place) is 1 per cent that of the final halo mass at $z=0$.

Similar results are found when we use modified versions of both the J08 and M12 models instead of B08.

5 SUMMARY AND CONCLUSIONS

In this work, we compare predictions from three models of merger times available in the literature to simulations of isolated mergers. We generate 50 simulations of single mergers between a satellite galaxy and a main halo at three redshift epochs, studying the evolution of the galaxy mass content and orbital angular momentum, as it is affected by dynamical friction. We probe a parameter space of different halo concentrations, merger mass ratios, orbital circularities, and orbital energies of galaxies.

We find that the implicit dependency on redshift in the models is not enough to account for variations as a function of redshift in our simulations. In particular, we find that prescriptions available in the literature significantly under-predict long timescales for mergers at high redshift. In a prescription derived from simulations of isolated mergers, this is found to be caused mainly by the lack of an explicit treatment of the evolution of halo concentration in satellite galaxies. On the other hand, in prescriptions derived from cosmological simulations, the disagreement is likely due to the fact that long merger times, as well as mergers with high initial orbital circularities, are under-represented.

Motivated by the effect of the evolution of halo concentration of satellites, we introduce a modification to the model derived from isolated mergers in the form $t_{\text{merger}}^{\text{mod}}(z) = (1+z)^{\alpha} t_{\text{merger}}$. With $\alpha=0.44$, the prescription improves significantly the predictions of merger times up to $\sim 20 t_{\text{dyn}}$ for mergers between $0 \leq z \leq 2$. We estimate that our proposed modification can lead up to a 25 per cent increase in the number of low mass galaxies in massive haloes, and a 10 per cent increase in the number of the most massive galaxies. This would worsen the disagreement between observations and predictions from semi-analytic models of galaxy evolution, as found in previous studies.

Precise predictions of merger timescales are a key ingredient in models of galaxy evolution. In a future work, we plan to investigate in detail the influence of our proposed modification, in the context of a realistic galaxy formation model coupled to N -body cosmological simulations.

ACKNOWLEDGEMENTS

ÁV and GDL acknowledge funding from ERC grant agreement n. 202781. SW acknowledges funding from ERC grant HIGHZ no. 227749. All simulations were run in CASPUR HPC facilities. The authors thank Volker Springel for making available the non-public version of the GADGET-3 code. This work has been partially supported by the Marie Curie Initial Training Network CosmoComp (PITN-GA-2009-238356), the PRIN-INAF09 project ‘‘Towards an Italian Network for Computational Cosmology’’, the PRIN-MIUR09 ‘‘Tracing the growth of structures in the Universe’’ and the PD51 INFN grant.

REFERENCES

- Behroozi P. S., Conroy C., Wechsler R. H., 2010, *ApJ*, 717, 379
- Benson A. J., 2005, *MNRAS*, 358, 551
- Berrier J. C., Stewart K. R., Bullock J. S., Purcell C. W., Barton E. J., Wechsler R. H., 2009, *ApJ*, 690, 1292
- Binney J., Tremaine S., 1987, *Galactic dynamics*, Binney, J. & Tremaine, S., ed.
- Boylan-Kolchin M., Ma C., Quataert E., 2008, *MNRAS*, 383, 93
- Bryan G. L., Norman M. L., 1998, *ApJ*, 495, 80
- Bullock J. S., Kolatt T. S., Sigad Y., Somerville R. S., Kravtsov A. V., Klypin A. A., Primack J. R., Dekel A., 2001, *MNRAS*, 321, 559
- Chandrasekhar S., 1943, *ApJ*, 97, 255
- Cox T. J., Jonsson P., Somerville R. S., Primack J. R., Dekel A., 2008, *MNRAS*, 384, 386
- De Lucia G., Blaizot J., 2007, *MNRAS*, 375, 2
- De Lucia G., Boylan-Kolchin M., Benson A. J., Fontanot F., Monaco P., 2010, *MNRAS*, 406, 1533
- De Lucia G., Fontanot F., Wilman D., Monaco P., 2011, *MNRAS*, 414, 1439
- De Lucia G., Weinmann S., Poggianti B. M., Aragón-Salamanca A., Zaritsky D., 2012, *MNRAS*, 423, 1277
- Guo Q., White S., Li C., Boylan-Kolchin M., 2010, *MNRAS*, 404, 1111
- Hernquist L., 1990, *ApJ*, 356, 359
- Jiang C. Y., Jing Y. P., Faltenbacher A., Lin W. P., Li C., 2008, *ApJ*, 675, 1095
- Liu L., Yang X., Mo H. J., van den Bosch F. C., Springel V., 2010, *ApJ*, 712, 734
- McCavana T., Micic M., Lewis G. F., Sinha M., Sharma S., Holley-Bockelmann K., Bland-Hawthorn J., 2012, *MNRAS*, 424, 361
- McGee S. L., Balogh M. L., Bower R. G., Font A. S., McCarthy I. G., 2009, *MNRAS*, 400, 937
- Moster B. P., Somerville R. S., Maulbetsch C., van den Bosch F. C., Macciò A. V., Naab T., Oser L., 2010, *ApJ*, 710, 903
- Navarro J. F., Frenk C. S., White S. D. M., 1997, *ApJ*, 490, 493
- Neto A. F., Gao L., Bett P., Cole S., Navarro J. F., Frenk C. S., White S. D. M., Springel V., Jenkins A., 2007, *MNRAS*, 381, 1450
- Springel V., 2005, *MNRAS*, 364, 1105
- Springel V., White S. D. M., Jenkins A., Frenk C. S., Yoshida N., Gao L., Navarro J., Thacker R., Croton D., Helly J., Peacock J. A., Cole S., Thomas P., Couchman H., Evrard A., Colberg J., Pearce F., 2005, *Nature*, 435, 629
- Villalobos Á., Helmi A., 2008, *MNRAS*, 391, 1806
- Weinmann S. M., van den Bosch F. C., Yang X., Mo H. J., Croton D. J., Moore B., 2006, *MNRAS*, 372, 1161
- Wetzell A. R., 2011, *MNRAS*, 412, 49